Molecular Modelling of Saccharides, 10[◇]
Studies on Ketoses, 12[◇◇]

The Electrostatic and Lipophilic Potential Profiles of α-Cyclofructin: Computation, Visualization and Conclusions

Stefan Immel and Frieder W. Lichtenthaler*

Institut für Organische Chemie der Technischen Hochschule Darmstadt,
Petersenstraße 22, D-64287 Darmstadt
Telefax: (internat.) +49(0)6151-166674

Received September 21, 1995

Key Words: Cyclofructohexaoside, molecular geometry of / Molecular lipophilicity pattern / Molecular electrostatic potential profile

On the basis of the color-coded visualization of molecular electrostatic (MEP) and lipophilicity potential (MLP) profiles, the structural differences and similarities between cyclo-β(1→2)-fructohexaoside (α-cyclofructin, **1**) and its backbone-derived 18-crown-6 ether and the cyclodextrins are outlined. Unlike α-cyclodextrin, α-cyclofructin exhibits no central cavity with which to form inclusion complexes. Rather, it has a pronounced "front/back" differentiation of hydrophobic and hydrophilic surface regions. In agreement with experimental observations, the MEP shows not only that the crown ether-type properties of α-cyclofructin are well-suited for the complexation of metal cations, but also that there is a pronounced regioselectivity for their incorporation.

Following the routes for the preparation of the cyclodextrins[2] from starch, the enzymatic degradation of inulin, a β(1→2)-linked fructofuranose-polysaccharide, yields a new type of cyclooligosaccharide represented by **1**, **2** and **3**, consisting of six to eight β(1→2)-linked fructofruanose residues[3,4]. In line with the simplified nomenclature recently proposed[5] for cyclooligosaccharides composed of sugar units other than glucose, which has already received some authoritative substantiation[6], **1** is appropriately designated as a cyclo-β(1→2)-fructohexaoside or, in brief, as α-cyclofructin[7] to emphasize its analogy to α-cyclodextrin. Accordingly, **2** and **3** are to be termed β- and γ-cyclofructin.

α-Cyclofructin **1**, the most readily accessible compound of this series, possesses as the macrocyclic core a unique 18-crown-6 skeleton onto which the furanoid rings are spiro-anellated in a propeller-like fashion. Due to this intriguing situation, we anticipated that a study of the molecular electrostatic and lipophilic features would be particularly informative of its ability to vie with the cyclodextrins for hydrophobic and electrostatic interactions.

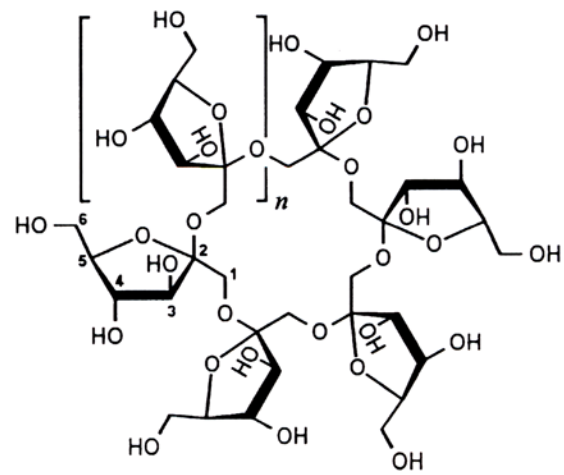

1 *cyclo*[D-Fruf β(1→2)]$_6$ (α-cyclofructin)
2 *cyclo*[D-Fruf β(1→2)]$_7$ (β-cyclofructin)
3 *cyclo*[D-Fruf β(1→2)]$_8$ (γ-cyclofructin)

Conformational Properties and Contact Surface of α-Cyclofructin

Solid state structural analysis of α-cyclofructin[4,8] revealed a molecular geometry with C_3 symmetry (cf. Figure 1). The two crystallographically different furanose rings adopt $E_3 \leftrightarrow {}^4T_3$ conformations with Cremer-Pople ring puckering parameters[9] (q = 0.383 Å/ϕ = 259.6° and q = 0.416 Å/ϕ = 261.7°) that are typical for β-D-fructofuranosyl residues. The propeller-like anellation requires the exocyclic 6-CH_2OH groups to be located on one side of the macrocycle pointing towards its outside, while the 3-hydroxyls cap the other side, with three out of the six hydroxyls forming a cycle of cooperative hydrogen bonds. The 18-crown-6 ether skeleton (Figure 1, right), laid bare of the α-cyclofructin,

[◇] Part 9: Ref.[1a].
[◇◇] Part 11: Ref.[1b].

  0947–3440/96/0101–0039 $ 10.00+.25/0

Figure 1. Ball and stick model representation of the solid-state structure of cyclo-β(1→2)-fructohexaoside (α-cyclofructin, **1**)[4,7] (left) and the 18-crown-6 skeleton **4** derived therefrom (right) including their contact surfaces in dotted form. Structures are shown perpendicular to the mean ring plane of the macrocycles. The α-cyclofructin is shown such that the 3- and 4-OH groups of the furanoid rings point towards the viewer, whereas the ring oxygen (O-5) and the primary 6-CH_2OH groups are directed towards the back. The orientation of the α-cyclofructin backbone is retained in the projection of the molecular geometry of the crown ether; oxygen atoms are shaded in both structures

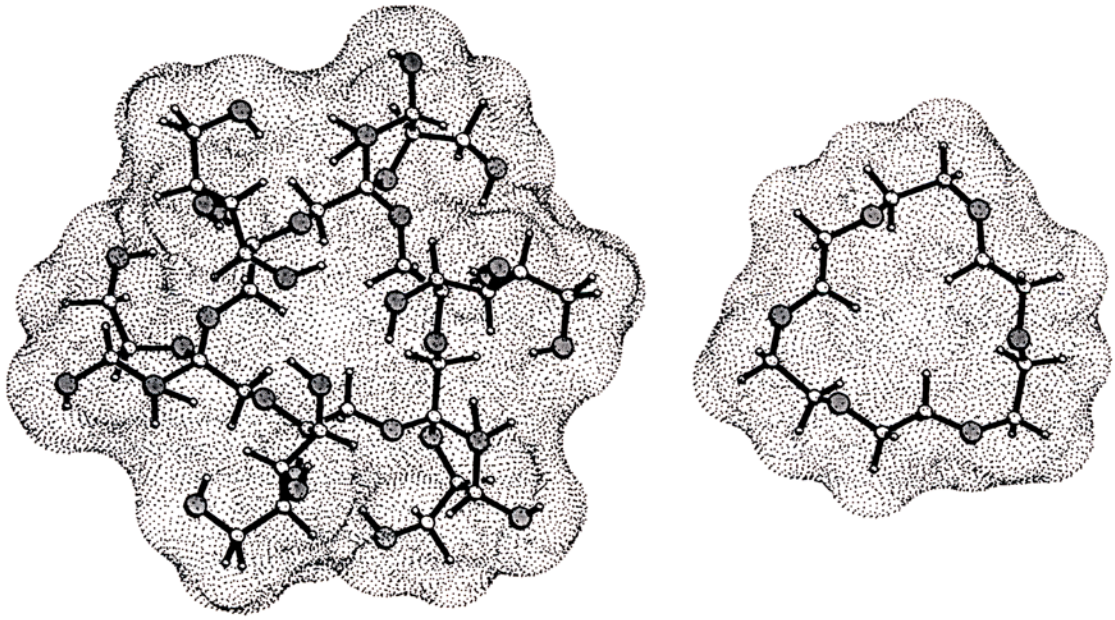

cyclo[D-Fruf β(1→2)]$_6$
1 (α-cyclofructin)

18-crown-6
4

Figure 2. Cross section plots through the contact surfaces of Figure 1 for α-cyclofructin **1** (left) and the 18-crown-6 ether **4** derived therefrom (right). Surface contours were obtained for a plane perpendicular to the macrocycle mean plane and successive 10° rotation steps around the geometrical center M, and were subsequently superimposed. As indicated on the left, the secondary 3-OH and 4-OH groups of the furanoid rings in **1** are at the bottom, whereas the ring oxygens and the 6-CH_2OH are located at the top of the contours. The molecular orientation of **4** corresponds to that of the α-cyclofructin **1** backbone with all ether oxygens pointing down and the methylene groups upward. The scale shown displays the approximate molecular dimensions obtained from these cross-section plots

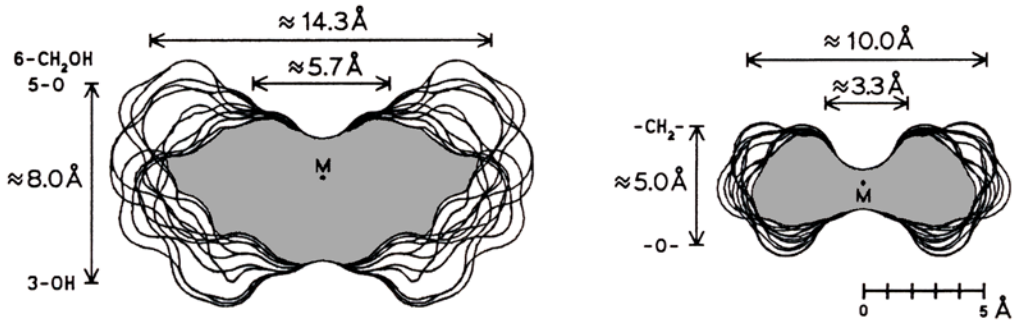

cyclo[D-Fruf β(1→2)]$_6$
1 (α-cyclofructin)

18-crown-6
4

exhibits a unique *gtgtgt* arrangement for the six O−CH_2−CH_2−O groupings, a conformation, which is realized neither in the unsubstituted 18-crown-6 (crystallizing in the *gtgggt* form[10]) nor in its metal ion complexes (favoring the all-*gauche* arrangement)[11]. Nevertheless, this *gtgtgt* conformation of the crown ether coincides with a local energy minimum and is not significantly changed upon full geometry optimization with the PIMM91 force-field[12].

A realistic model for the spatial dimensions and the accessibility of molecular regions for solvent molecules like water, for example, is provided by molecular surfaces. Accordingly, using the well-suited MOLCAD program[13],

contact surfaces[14], roughly equivalent to the solvent-accessible surfaces[15], were generated for both the crystal structure geometry of α-cyclofructin[4,8] (Figure 1, left) and its underlying 18-crown-6 backbone portion, (Figure 1, right). As is clearly evident, the α-cyclofructin **1** is devoid of a central cavity, a fact that is even more clearly demonstrated by the cross section plots through the surface given in Figure 2. In Figure 2, not a cavity, but rather a small and shallow surface groove is observed on either side of the α-cyclofructin macrocycle. This also holds true for the 18-crown-6 ether **8** in the α-cyclofructin-derived conformation, with a somewhat deeper surface dent in its molecular center.

The absence of a central cavity in α-cyclofructin and the loss of the torus-like shape well-established for α-cyclodextrin[2], α-cyclomannin, and α-cyclogalactin[5a] precludes the formation of inclusion compounds. It is noteworthy though, that the effective molecular dimensions displayed by the surface cuts of α-cyclofructin such as the macrocycle diameter of ≈14.3 Å and a thickness of ≈8.0 Å correspond closely to the size parameters of α-cyclodextrin (diameter: ≈14.2 Å, torus height: ≈8.0 Å[5]). The apparent molar volume $^{\Phi}V$ of α-cyclofructin as determined from the volume enclosed by the surface is calculated to be approximately 980−985 Å^3 (≈160−165 Å^3 per fructose unit and ≈590−595 cm^3/mol), and thus also corresponds closely to the volume of 970−975 Å^3 calculated for α-CD[5]. The experimental value of $^{\Phi}V \approx 1010$ Å^3 found for α-CD in aqueous solution[16] indicates its central cavity to be − at least to a large extent − filled with water molecules. Volumes of similar magnitude are therefore to be expected for **1**.

Figure 3. MOLCAD-program generated molecular lipophilicity patterns (MLP) projected onto the contact surfaces of cyclo-[Fru*f*β(1→2)]$_6$ (**1**, α-cyclofructin, left each) and 18-crown-6 ether (**4**, right) in the same conformation (*gtgtgt* arrangement of O−CH_2−CH_2−O units) as realized in the spiro-substituted macrocycle **1**. For visualization, a two-color-code graded into 32 shades was used to map the computed values onto the contact surface, i.e. 16 color shades ranging from dark blue (most hydrophilic surface areas) over light blue to full yellow (most hydrophobic regions). Another 16 shadings (light blue to brown) indicate iso-contour lines in between the former color scale, thus allowing a more quantitative assessment of the relative hydrophobicity on different surface regions. The orientation of **1** was chosen such that the secondary hydroxyl groups of the furanoid ring (3-OH and 4-OH) are directed towards the viewer, whereas the C_5−O_5/C_6−O_6 fragments point to the back (cf. Figure 1). The view of **4** corresponds to the orientation of the backbone in **1**, the ether oxygens facing the front and the methylene groups pointing towards the back. In the lower picture, the hydrophilic front half of the molecular surfaces has been removed to provide an inside view of the hydrophobic (yellow) back

Figure 4. Molecular electrostatic potential (MEP) profiles on the contact surface of α-cyclofructin (**1**, left) and 18-crown-6 ether (**4**, right). The 16-color-code ranging from violet (most negative potential) to red (most electropositive potential) was applied in relative terms for each molecule separately. The molecular orientations and the modes of viewing correspond to Figures 1 and 3, the lower entry visualizing the back surface properties of **1** and **4** by removal of their front halves

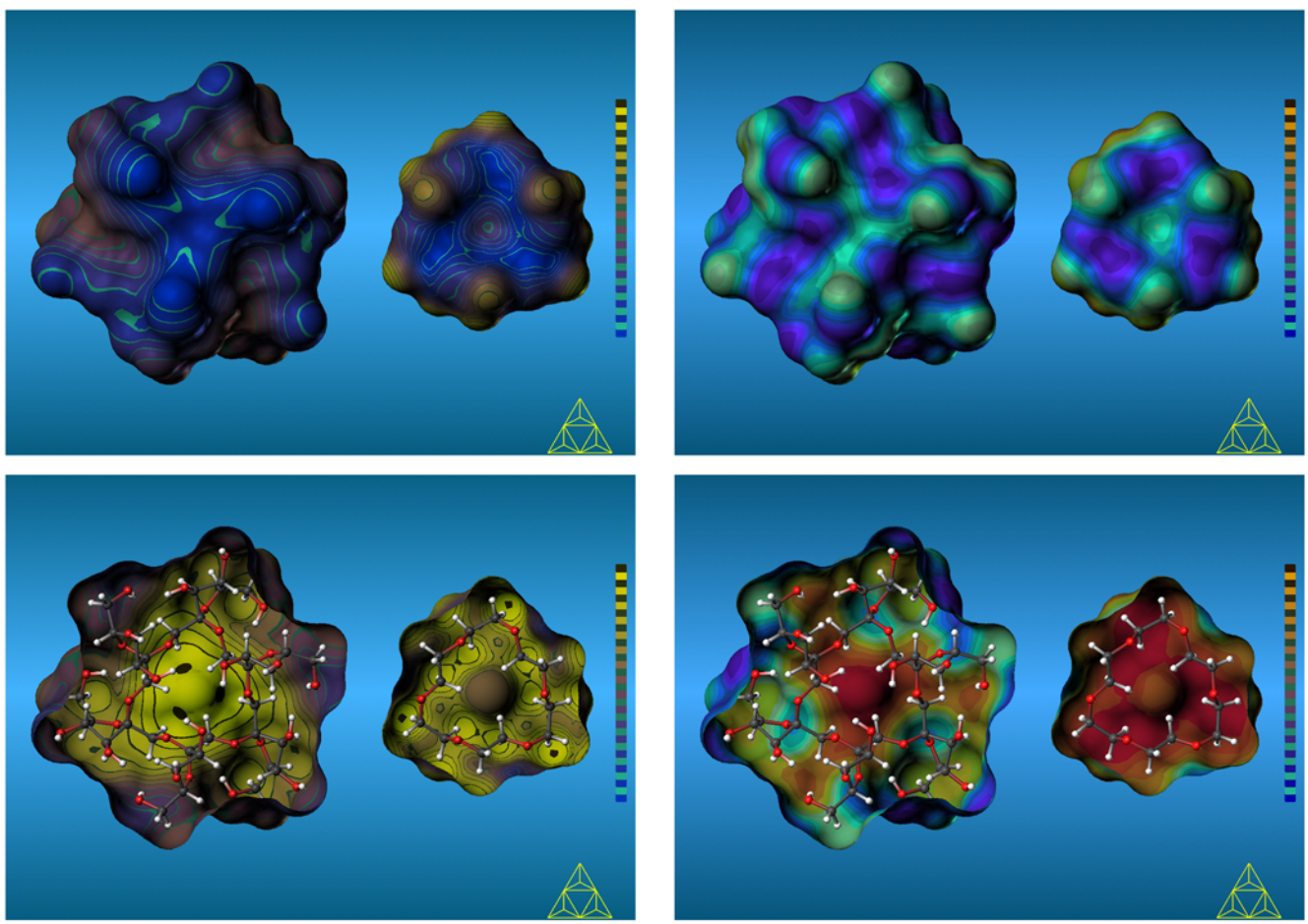

As the characteristic crown ether backbone in the central part of α-cyclofructin binds cations via charge-dipole electrostatic interactions[17] and may be surmised to exhibit sandwich-type binding of neutral molecules through hydrophobic interactions – in very much the same way as cyclodextrins enclose guest molecules into their hydrophobic cavities – it was of interest to generate the lipophilicity pattern of **1** as well as its electrostatic profile.

Lipophilicity Pattern of α-Cyclofructin

Generation of the *M*olecular *L*ipophilicity *P*attern (MLP)[18], particularly when projected onto the contact surface in color-coded form[19] as provided by the MOLCAD program[13], allows to readily identify hydrophilic and hydrophobic surface regions even for large molecules. For the cyclodextrins[5,20] and α-cyclomannin[5a], the most hydrophobic surface areas are located inside their cavities, providing ample evidence for the hydrophobic effect to be of fundamental importance for the formation of inclusion complexes. In the case of α-cyclogalactin[5a], the surface parts corresponding to the inner cavity of α-cyclodextrin have been turned inside-out, and, consequently, the central hole becomes more hydrophilic than the outer surface parts.

Application of the very same methodology – calculation and visualization of the MLP in a 32-color-code – to α-cyclofructin (**1**) indicates a distinctive differentiation of hydrophilic and hydrophobic surface regions with regard to its "front" and "back" (Figure 3, left). The 3-OH and 4-OH of each fructofuranosyl moiety, as well as the primary O-1, involved in the intersaccharidic linkages, are located on the same side of the molecule, that is, the "front" (pictured in Figure 3). This causes this surface region to be highly hydrophilic. The areas located at the opposite side are associated with the 1- and 6-methylene groups and the $O_5-C_5-H_5$ fragments that contribute to an obviously more hydrophobic surface. The same trend is observed for the 18-crown-6 core in the *gtgtgt* conformation (Figure 3, right). The striking correspondence of opposite side-located hydrophilic and hydrophobic regions is caused by the spatial separation of the surface parts, all oxygens being oriented to one side and the CH_2CH_2 units to the other.

Accordingly, in aqueous solution, the hydrophilic molecular parts of α-cyclofructin as well as its crown ether core **4** should be more affected by solvation and hydrogen bonding interactions than the opposite water-repellent (hydrophobic) regions. Although hydrophobic interactions are generally not very strong[21], the accumulation of lipophilic regions on only one side of the disk-shaped molecule may well give rise to self-assemblies that are dependent on the solvent: in aqueous solution the two hydrophobic sides could merge to generate a dimer with hydrophilic outside surface areas, hence easily solvated by water. In organic solvents, however, aggregation of the hydrophilic sides is more likely to cause the formation of a dimer with an essentially hydrophobic outside. Solubility studies, that would provide information on this, are being contemplated. On the other hand, the packing of the α-cyclofructin molecules in the crystal lattice[8] is characterized by regular columns in which the α-cyclofructin discs are stacked normally, with the hydrophilic side of one molecule facing the hydrophobic side of the next. This stacking is obviously brought about by cooperative, interdisc hydrogen bonds of the 6-OH···4′-OH···O-5-type, three up and three down, that are comparatively tight (6–4···O-4′ distance 1.99 Å). This behaviour is substantially different from that of the cyclodextrins, which tend to assemble in head-to-head dimers through elaboration of an intense hydrogen bonding network between the secondary hydroxyl groups of two adjacent CD-tori.

The Electrostatic Potential Profile of α-Cyclofructin

Crown ethers are well-known for their ability to complex a large variety of metal cations by chelate coordination through their ether-type oxygen atoms[11]. Since the stability of these complexes can be attributed mainly to strong electrostatic interactions between their C–O bond dipoles and the cation[11], the *M*olecular *E*lectrostatic *P*otential (MEP) profile[22] of α-cyclofructin should be more relevant for assessment of its chemical properties than the MLP is. Thus, the MEP profiles of α-cyclofructin (**1**) and its 18-crown-6 backbone **4** were calculated from the PIMM91 partial atomic charges[12] of the fully optimized geometries, and were transferred into a 16-color-code by projection of the computed values onto the corresponding surfaces. They reveal even further similarities between both compounds: the negatively charged O-1, O-3, and O-4 atoms of the fructofuranose portions of **1** as well as the oxygens of the crown ether **4** in the *gtgtgt* conformation are situated on the hydrophilic sides of the disks, and thus highly negative electrostatic potentials (≈–15 to –25 kcal/mol) are computed for these surface regions. Moreover, the opposite hydrophobic areas made up by the CH_2 groups pointing towards the center surface dent, are characterized by high positive potentials. The striking similarities between both structures allows the reasonable assumption that their physico-chemical properties based on electrostatic interactions should closely correspond each other.

Indeed, there is overwhelming NMR evidence for the complexation of metal cations by α-cyclofructin[17] and its permethylated derivative[23] in aqueous solution as well as in organic solvents. Despite the association constants for α-cyclofructin being approximately two orders of magnitude smaller than those measured for the corresponding 18-crown-6[23], the effects observed suggest strong binding of the cations Pb^{2+}, Ba^{2+}, K^+, Rb^+, and Cs^+, for example; while Li^+, Na^+, and Ca^{2+} interact only very weakly with α-cyclofructin[17,23]. On the basis of induced-shift differences in the ^{1}H-NMR spectra of the K^+ and Ba^{2+} complexes – both cations have approximately the same size but different charges, and thus, should level off the effect of conformational changes of the host – it becomes obvious that the oxygen atoms O-1 and, in particular, O-3 are involved in capturing cations[23]. In a strict sense these considerations are only valid if both complexes exhibit identical or closely similar conformations. Since low-temperature NMR revealed different types of symmetry for both geometries (C_2 symmetry for Ba^{2+} and C_3 symmetry for K^+),

conclusions based on the charge-induced shifts may be misleading[23]. This notwithstanding, the MEP profile of α-cyclofructin, as depicted in Figure 4, strongly supports the proposed regioselectivity of metal cation incorporation: the highly negative electrostatic potentials around the O-1, O-3, and O-4 atoms act as a long-range trap for the cations, the side specificity being even more enhanced by the repulsive positive potentials on the opposite side. Direct proof for these models was obtained from solid-state structure analysis of the permethylated α-cyclofructin · $Ba(SCN)_2$ complex, indicating a 10-fold coordination of the Ba^{2+} ion by all O-1 atoms and four out of six of the 3-OMe groups (long-range interaction with the SCN anion might even increase the coordination number to 11)[23]. The results point out one probable mechanism for the complex formation: simultaneous or successive rotation of the spiro-anellated fructofuranosyl residues – in the sense of the 3-OMe groups moving from the center axis towards the outside of the molecule – opens a center pocket of high electronegative character. Trapping and inclusion of the cation by long-range strong electrostatic forces leads to the constitution of the complex, whereby the resulting symmetry of the adduct depends on the strength of the Coulomb interactions (i.e. the charge of the cations)[23] and the type of preferred coordination.

In conclusion, both the MLP and the MEP patterns clearly illustrate the crown ether-type properties of α-cyclofructin with respect to capturing and complexing metal ions; the results obtained agree with experimental data, and the functional groups of α-cyclofructin involved in cation complexation are unequivocally identified. In relation to the inclusion complex formation of cyclodextrins that is mainly governed by hydrophobic interactions, the α-cyclofructin represents an interesting complementary example to study electrostatic interactions of carbohydrates with metal cations. Studies of the larger ring homologs, cyclofructoheptaoside **2** and the octaoside **3** may be even more engaging because their more well-defined surface dents and small cavities are apt to provide both electrostatic complexing and hydrophobic inclusion properties.

We thank Prof. Dr. *J. Brickmann*, Technische Hochschule Darmstadt, for providing us the MOLCAD molecular modelling software package and his computational facilities.

Experimental

Molecular Surfaces, Molecular Electrostatic and Lipophilicity Patterns: Calculation of the molecular contact surfaces, MEPs, and MLPs was carried out by using the MOLCAD[13] molecular modelling program and texture mapping[19]. Scaling of the hydrophobicity profiles and electrostatic patterns was performed in arbitrary units and in relative terms for each molecule separately, and no absolute values are displayed. Color graphics were photographed from the computer screen of a SILICON-GRAPHICS workstation.

[1] [1a] Part 9: F. W. Lichtenthaler, S. Immel, *Liebigs Ann.* **1996**, 27–37 (preceding paper). – [1b] Part 11: F. W. Lichtenthaler, S. Hahn, F. J. Flath, *Liebigs Ann.* **1995**, 2081–2088.
[2] [2a] W. Saenger, *Angew. Chem.* **1980**, *92*, 343–361; *Angew. Chem. Int. Ed. Engl.* **1980**, *19*, 344–362. – [2b] G. Wenz, *Angew. Chem.* **1994**, *106*, 851–870; *Angew. Chem. Int. Ed. Engl.* **1994**, *33*, 803–822.
[3] M. Kawamura, T. Uchiyama, T. Kuramoto, Y. Tamura, K. Mizutani, *Carbohydr. Res.* **1989**, *192*, 83–90.
[4] T. Uchiyama, *Stud. Plant Sci. (Inulin and Inulin-Containing Crops)* **1993**, *3*, 143–148.
[5] [5a] F. W. Lichtenthaler, S. Immel, *Tetrahedron Asymmetry* **1994**, *5*, 2045–2060. – [5b] S. Immel, J. Brickmann, F. W. Lichtenthaler, *Liebigs Ann.* **1995**, 929–942.
[6] *Cyclodextrin News* (Ed.: S. Szejtli), Cyclolab FDS Publ., Budapest, **1994**, *9*, 41–42.
[7] The term "cyclofructin" is considered to be the generic name for all cyclooligosaccharides composed of fructoses, irrespective of their intersaccharidic link-up. Aside from the β(1→2)-interconnection realized in **1**, the anomerically inverted α(1→2)-linked cyclofructins are conceptually intriguing, as the furanoid ring presumably adopts the E_2 conformation (i).
Other, potentially interesting cyclofructin linkage isomers are those having fructopyranose units, e.g. the cyclo[D-Fru*p* β(1→2)]$_6$, the pyranoid analog of **1** (ii), and the cyclo-α(2→5)-fructohexaoside (iii), in which the $^5C_2$ conformation, as depicted in (iii), is surmised to be substantially distorted, since two adverse effects are to be counterbalanced: operation of the anomeric effect entailing adoption of the $^5C_2$ conformation as depicted in (iii), and steric congestion in the macrocyclic ring by the axially oriented 3-OH and 4-OH groups.

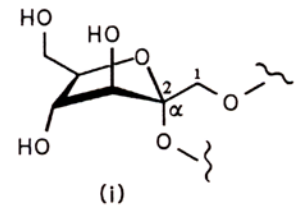

(i)

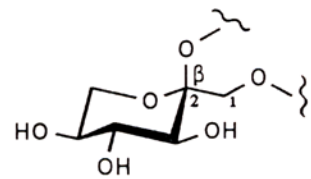

(ii)

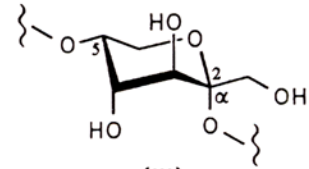

(iii)

[8] M. Sawada, T. Tanaka, Y. Takai, T. Hanafusa, T. Taniguchi, M. Kawamura, T. Uchiyama, *Carbohydr. Res.* **1991**, *217*, 7–17.
[9] [9a] D. Cremer, J. A. Pople, *J. Am. Chem. Soc.* **1975**, *97*, 1354–1358. – [9b] G. A. Jeffrey, R. Taylor, *Carbohydr. Res.* **1980**, *81*, 182–183.
[10] [10a] J. D. Dunitz, P. Seiler, *Acta Crystallogr., Sect. B*, **1974**, *30*, 2339–2341. – [10b] E. Maverick, P. Seiler, B. Schweizer, J. D. Dunitz, *ibid.* **1980**, *36*, 615–620.
[11] [11a] C. J. Pedersen, *J. Am. Chem. Soc.* **1967**, *89*, 2495–2496; 7017–7036. – [11b] J. W. H. M. Uiterwijk, S. Harkema, D. Feil, *J. Chem. Soc., Perkin Trans. 2*, **1987**, 721–731.
[12] [12a] H. J. Lindner, *Closed Shell PI-SCF-LCAO-MO Molecular Mechanics Program (PIMM91)*, Technische Hochschule Darmstadt, **1988**. – [12b] A. E. Smith, H. J. Lindner, *J. Comput.-Aided Mol. Des.* **1991**, *5*, 235–262.
[13] [13a] J. Brickmann, *MOLCAD – MOLecular Computer Aided Design*, Technische Hochschule Darmstadt, **1992**. The major part of the MOLCAD program is included in the SYBYL package of TRIPOS Associates, St. Louis, USA. – [13b] J. Brickmann, *J. Chim. Phys.* **1992**, *89*, 1709–1721. – [13c] M. Waldherr-Teschner, T. Goetze, W. Heiden, M. Knoblauch, H. Vollhardt, J. Brickmann, in: *Advances in Scientific Visualization* (Eds.: F. H. Post, A. J. S. Hin), Springer Verlag, Heidelberg, **1992**, pp. 58–67. – [13d] J. Brickmann, T. Goetze, W. Heiden, G. Moeckel, S. Reiling, H. Vollhardt, C.-D. Zachmann, *Interactive Visualization of Molecular Scenarios with MOLCAD/SYBYL*, in: *Insight and Innovation in Data Visualization* (Ed.: J. E. Bowie), Manning Publications Co., Greenwich, **1994**, pp. 83–97.

[14] [14a] F. M. Richards, *Ann. Rev. Biophys. Bioeng.* **1977**, *6*, 151–176; *Carlsberg. Res. Commun.* **1979**, *44*, 47–63. – [14b] M. L. Connolly, *J. Appl. Cryst.* **1983**, *16*, 548–558; *Science* **1983**, *221*, 709–713.
[15] B. Lee, F. M. Richards, *J. Mol. Biol.* **1971**, *55*, 379–400.
[16] H. Nomura, S. Koda, K. Matsumoto, Y. Miyahara, *Stud. Phys. Theor. Chem.* **1983**, *27*, 151–163.
[17] [17a] N. Yoshie, H. Hamada, S. Takada, Y. Inoue, *Chem. Lett.* **1993**, 353–356. – [17b] T. Uchiyama, M. Kawamura, T. Uragami, H. Okuno, *Carbohydr. Res.* **1993**, *241*, 245–248.
[18] W. Heiden, G. Moeckel, J. Brickmann, *J. Comput.-Aided Mol. Des.* **1993**, *7*, 503–514.
[19] M. Teschner, C. Henn, H. Vollhardt, S. Reiling, J. Brickmann, *J. Mol. Graphics* **1994**, *12*, 98–105.
[20] Parts of this work are contained in a review: F. W. Lichtenthaler, S. Immel, *Internat. Sugar J.* **1995**, *97*, 12–22.
[21] W. Blokzijl, J. B. F. N. Engberts, *Angew. Chem.* **1993**, *105*, 1610–1648; *Angew. Chem. Int. Ed. Engl.* **1993**, *32*, 1545–1579.
[22] [22a] P. K. Weiner, R. Langridge, J. M. Blaney, R. Schaefer, P. A. Kollman, *Proc. Natl. Acad. Sci. USA* **1982**, *79*, 3754–3758. – [22b] C. E. Dykstra, *Chem. Rev.* **1993**, *93*, 2339–2353.
[23] Y. Takai, Y. Okumura, T. Tanaka, M. Sawada, S. Takahashi, M. Shiro, M. Kawamura, T. Uchiyama, *J. Org. Chem.* **1994**, *59*, 2967–2975.

[95265]